Journal of Russian Laser Research, Volume 20, Number 2, 1999

NEW METHODS OF X-RAY REFLECTOMETRY OF SOLIDS AND SOLID THIN FILMS

R. M. Feshchenko, I. V. Pirshin, A. G. Touryanski, and A. V. Vinogradov

P. N. Lebedev Physical Institute, Russian Academy of Sciences, Leninskii Pr. 53, Moscow 117924, Russia
e-mails: vinograd@sci.lebedev.ru rusl@sci.lebedev.ru

Abstract

X-ray reflectometry makes it possible to determine optical constants of materials in the corresponding range of wavelengths and the thickness of thin films on the basis of measurements of reflection coefficients in relation to the grazing angle. New reflectometry methods based on measurements of either the derivatives with respect to the grazing angle or the ratios of reflection coefficients for two characteristic wavelengths are suggested. Calculations and measurements indicate that the method suggested makes it possible to enhance the sensitivity of reflectometry and the accuracy of measuring the optical constants. Practical implementation of the method is based on an unconventional system of selecting monochromatic beams with the use of semitransparent crystals. The results of reflectometry studies of GaAs single crystals and a $Ga_{0.25}Si_{0.75}$ – Si multilayer structure on a Si substrate are reported.

1. Introduction

Beginning in the 1950s, x-ray reflectometry (i.e., study of the dependence of the reflectivity of x-ray radiation on the grazing angle) has come to be regarded as an efficient and universal method for determining the x-ray optical constants, density, and other material's parameters in thin films and bulk solids [1–4]. It is noteworthy that at that time the methods of surface treatment and coating did not ensure the surface flatness and roughness parameters required for x-ray reflectometry, which resulted in marked discrepancies between the experimental and theoretical data. In order to alleviate these discrepancies, complex speculative models of the transition surface layer have been developed. At present, the technological problems are largely solved. In particular, in large-scale production of semiconductor wafers it is possible to attain an r.m.s deviation of the relief from planarity of 0.3–0.4 nm; with special methods of treatment, this deviation can be reduced to 0.1–0.2 nm. Even smoother substrates are often used for fabrication of reflective elements in x-ray optical systems.

With the aforementioned parameters of roughness, the use of the Fresnel formulas becomes justified and, basically, ensures the possibility of determining the characteristics of the medium and the near-surface layer.

The current progress in the field of reflectometry, especially as applied to ultrathin nanodimensional films, can be inferred from [5, 7].

However, two types of problems that are becoming increasingly more urgent motivate us to turn our attention again to the analysis of the ultimate potentialities of x-ray reflectometry as a method for studying materials in the form of solid thin films and bulk solids. First, we have in mind the extension of multilayer optical methods to the short-wavelength region. Let us consider, for example, the problem of developing x-ray optical systems with submicron resolution. The most important applications correspond to the wavelength range of $\lambda < 45$ Å. At the same time, the reflectivity of multilayer mirrors in this region at normal incidence is 15 % (the highest ever value reported in [8]). At present, this is an outstanding result; however, it is 2–3 times smaller than the theoretical limit.

Translated from a manuscript submitted December 15, 1998.

 1071-2836/99/2002-0136$22.00

Apparently, in order to attain this limit, one has to study the processes of layer formation in multilayer coatings. Furthermore, we are dealing here with layer thicknesses $\leq \lambda/4$, i.e., in this case, we are concerned with the study of films with a thickness of about 11 Å.

The other type of problem is related to the physics and technology of ultrashort laser pulses with picosecond and femtosecond durations. When this pulsed radiation is focused onto the solid surface, it gives rise to x-ray pulses of identically short duration. By optimizing the experiment's geometry and by using two consecutive laser pulses, the first of which generates a pre-plasma and the second (of higher intensity) of which accelerates electrons, one can realize the situation where the major fraction of radiation is confined in characteristic x-ray lines with energies of 10 keV and higher [9]. Thus, we can state that there is an entirely new source of radiation in the wavelength range widely used for structural studies. Radical dissimilarities of this source from, for example, x-ray tubes consist of short-pulse duration ($\sim 10^{-12}-10^{-14}$ s), extremely high intensity of radiation, and fairly small size of the emitting region ($\sim 10^{-3}-10^{-4}$ cm). At the same time, in contrast to a synchrotron, the new source (at least, in outlook) a compact laboratory unit and does not require a vacuum. Obviously, these sources will make it possible to perform structural studies at a completely new level of temporal and spatial resolutions. However, implementation of the merits of these sources will depend to a large extent on the sensitivity of the x-ray optical systems used.

In connection with the above, we consider here certain new methods of measurement and processing of results that will make it possible to enhance the accuracy, reliability, and sensitivity of x-ray reflectometry when being applied to bulk solids and solid thin films.

2. Single-Wavelength Method. Direct and Differential Measurements

2.1. Direct Measurements

For completeness of the presentation, we first provide certain information on the conventional x-ray reflectometry [10]. Experimental determination of materials' optical properties in the x-ray region of the spectrum is based on measurements of the angular dependence of the reflection coefficient; this dependence, in view of the Fresnel formulas, can be given by

$$R = |r|^2, \qquad r = \frac{\sqrt{x^2+z}-x}{\sqrt{x^2+z}+x}, \qquad x = \sin\theta, \qquad z = \varepsilon - 1 = -\delta + i\beta, \tag{1}$$

where θ is the grazing angle and $\varepsilon = 1 - \delta + i\beta$ is the dielectric constant of the material. Formula (1) is valid, in the strict sense, for s-polarization; however, in the x-ray region of the spectrum it also holds for p-polarization owing to the fact that the grazing angle is small.

Determination of δ and β is performed by fitting the two parameters in accordance with formula (1) in the experimental reflection-coefficient dependence $R(\theta)$. Figure 1 shows the dependences $R(\theta)$ for a number of materials of interest for the physics of semiconductors and for short-wavelength x-ray optics.

If a film has been deposited onto a substrate with known optical constants δ and β, the thickness d and the optical constants δ_1 and β_1 of the film can also be determined by measuring the reflection coefficient of the film–substrate system and comparing the result with the corresponding theoretical formula. Should the need arise, the fitting is performed for all three parameters d, δ, and β [5, 6]. Figures 2–4 show the families of curves describing the angular dependence of the reflection coefficient for the following film–substrate systems:

— Ni on Si single crystal (Fig. 2),

— GeO on Ge single crystal (Fig. 3),

— SiO_2 on Si single crystal (Fig. 4).

It is evident, in particular, that an appreciable sensitivity of the reflection coefficient to the film's thickness for various materials begins with thicknesses of about 10–30 Å or more.

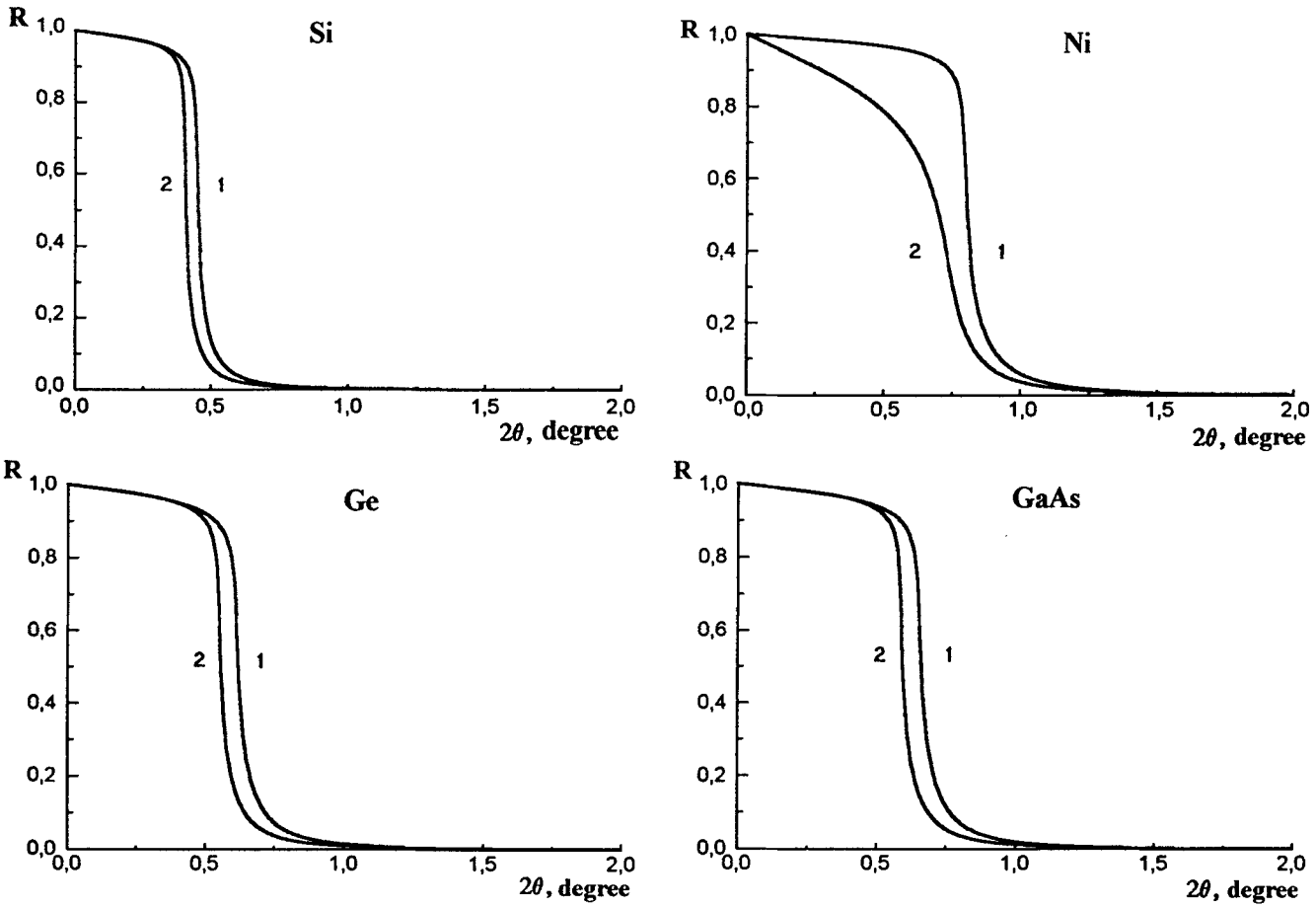

Fig. 1. Examples of the Fresnel reflection coefficients for several materials. The calculations were performed for wavelengths of 1.54 Å (curve 1, the characteristic copper line CuK_α) and 1.39 Å (curve 2, the characteristic line CuK_β).

2.2. Differential Method

We now consider the reflection-coefficient derivative with respect to the grazing angle. We use (1) to arrive at[1]

$$\frac{1}{R}\frac{dR}{d(\sin\theta)} = \frac{1}{r}\frac{dr}{dx} + \frac{1}{r^*}\frac{dr^*}{dx} = -2|r|^2\left\{\frac{1}{\sqrt{x^2+z}} + \frac{1}{\sqrt{x^2+z^*}}\right\}, \qquad x = \sin\theta\,. \tag{2}$$

We introduce the dimensionless angle as

$$t = \frac{x^2-\delta}{\beta}; \qquad x = \sqrt{\beta t+\delta}, \qquad -\frac{\delta}{\beta} \le t \le \frac{1-\delta}{\beta}\,. \tag{3}$$

We may then verify that formula (2) for the derivative can be written as

$$\frac{1}{R}\frac{dR}{dx} = -\frac{2}{\sqrt{\beta}}f(t)\,, \tag{4}$$

$$f(t) = \frac{1}{\sqrt{t+i}} + \frac{1}{\sqrt{t-i}} = \sqrt{2\frac{t+\sqrt{t^2+1}}{t^2+1}}\,. \tag{5}$$

[1]For detailed analysis of the Fresnel formulas, see [11].

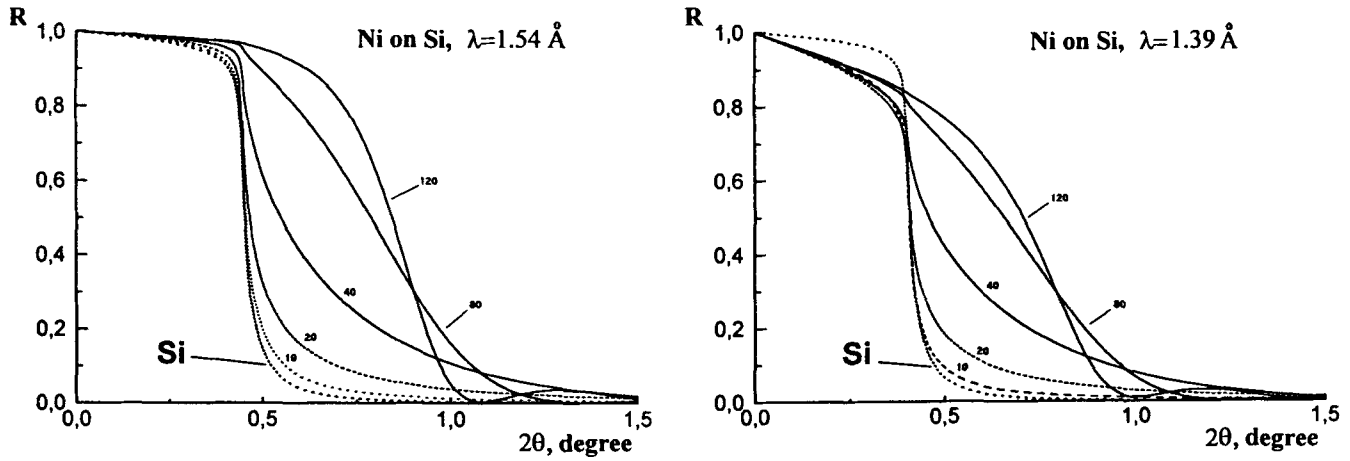

Fig. 2. Examples of the Fresnel reflection coefficients for Ni films on Si monocrystal. The numbers at the curves correspond to the films' thicknesses in Å.

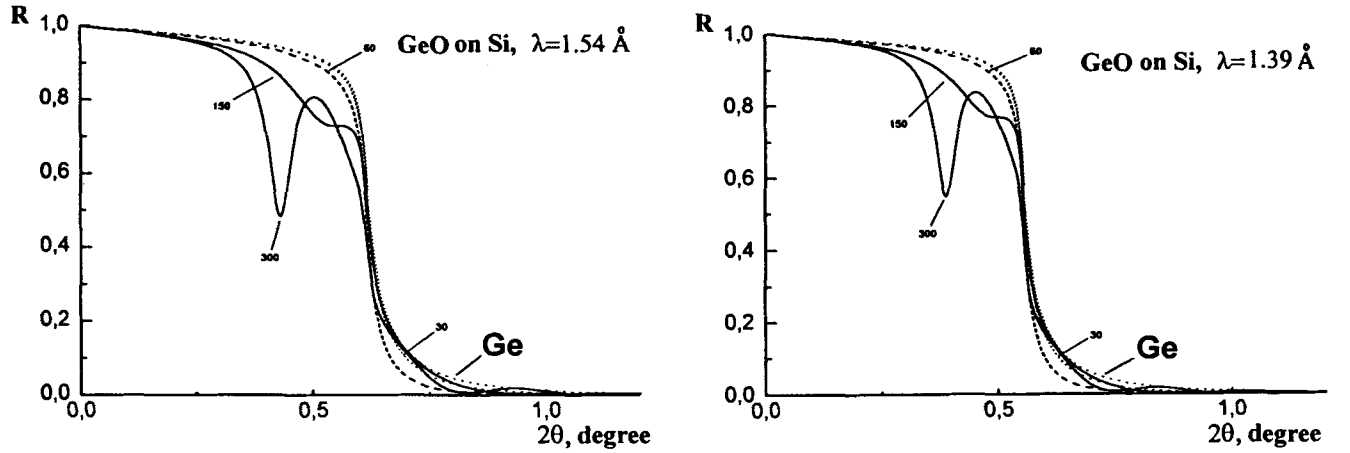

Fig. 3. Examples of the Fresnel reflection coefficients for GeO films on Ge monocrystal. The numbers at the curves correspond to the films' thicknesses in Å.

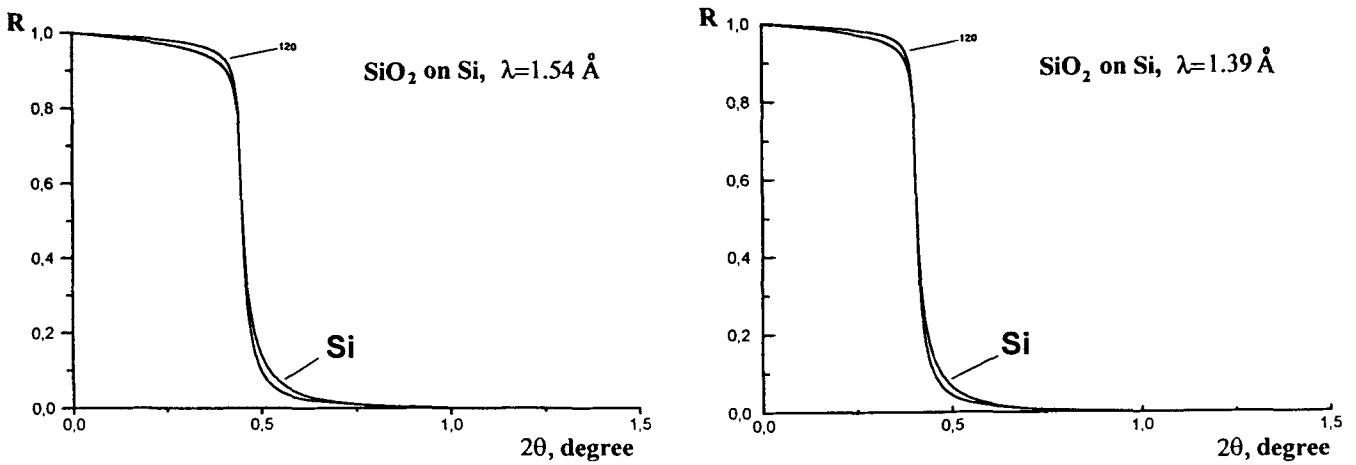

Fig. 4. Examples of the Fresnel reflection coefficients for SiO_2 films on Si. The number at the curve corresponds to the film's thickness in Å.

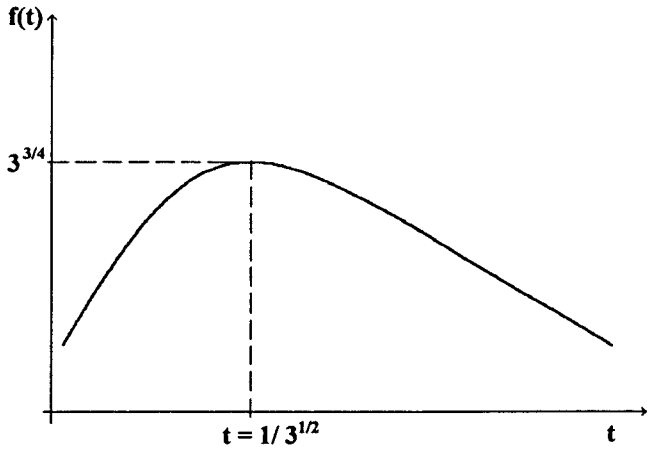

Fig. 5. A plot of the universal function $f(t)$ [see formula (5)].

It follows from formulas (4) and (5) that the logarithmic derivative of the reflection coefficient $\frac{1}{R}\frac{dR}{dx}$ is a universal function of the variable t [see (3)], i.e., this derivative is the same for all materials. A plot of the function $f(t)$ is shown in Fig. 5. For $t_0 = 1/\sqrt{3} \simeq 0.58$, this function has a maximum $f_0 = f\left(\frac{1}{\sqrt{3}}\right) = 3^{3/4} \simeq 2.28$.

Obviously, in view of such a universality, it is more convenient to use the derivative $\frac{1}{R}\frac{dR}{dx}$ (rather than the reflection coefficient R) in determining the optical constants λ and β of the material. We now dwell briefly on the properties following from formulas (4) and (5).

We note first of all that the existence of a maximum of the function $f(t)$ makes it possible to introduce a simple test for the existence of the phenomenon of total external reflection in absorbing materials and to provide a clear definition of the critical angle.

In fact, it is reasonable to assume that, in the material under consideration, we have the effect of total external reflection of x-rays if there is a maximum in the angular dependence of $\frac{1}{R}\frac{dR}{d(\sin\theta)}$. The grazing angle corresponding to the maximum of this dependence may be naturally identified with the critical angle of total external reflection. Thus, in accordance with (3) and Fig. 4, the total external reflection is realized if

$$-\delta < \frac{\beta}{\sqrt{3}} < 1 - \delta \qquad \text{or} \qquad [\operatorname{Re}\varepsilon - 1] < \frac{\operatorname{Im}\varepsilon}{\sqrt{3}} < \operatorname{Re}\varepsilon\,. \tag{6}$$

In this case, the critical angle is given by

$$\sin^2\theta_0 = \delta + \frac{\beta}{\sqrt{3}}\,. \tag{7}$$

In the absence of absorption (i.e., for $\beta = 0$), formulas (6) and (7) are transformed into the known conditions for the total external reflection for nonabsorbing materials [12]

$$\sin^2\theta_0 = \delta\,,$$

with $0 < \delta < 1$.

We note next that determination of optical constants is greatly simplified if the experimental dependence of $\frac{1}{R}\frac{dR}{d(\sin\theta)}$ on θ is known. In fact, let the maximum of the logarithmic derivative

$$A_m = \max\left[-\frac{1}{R}\frac{dR}{d(\sin\theta)}\right]$$

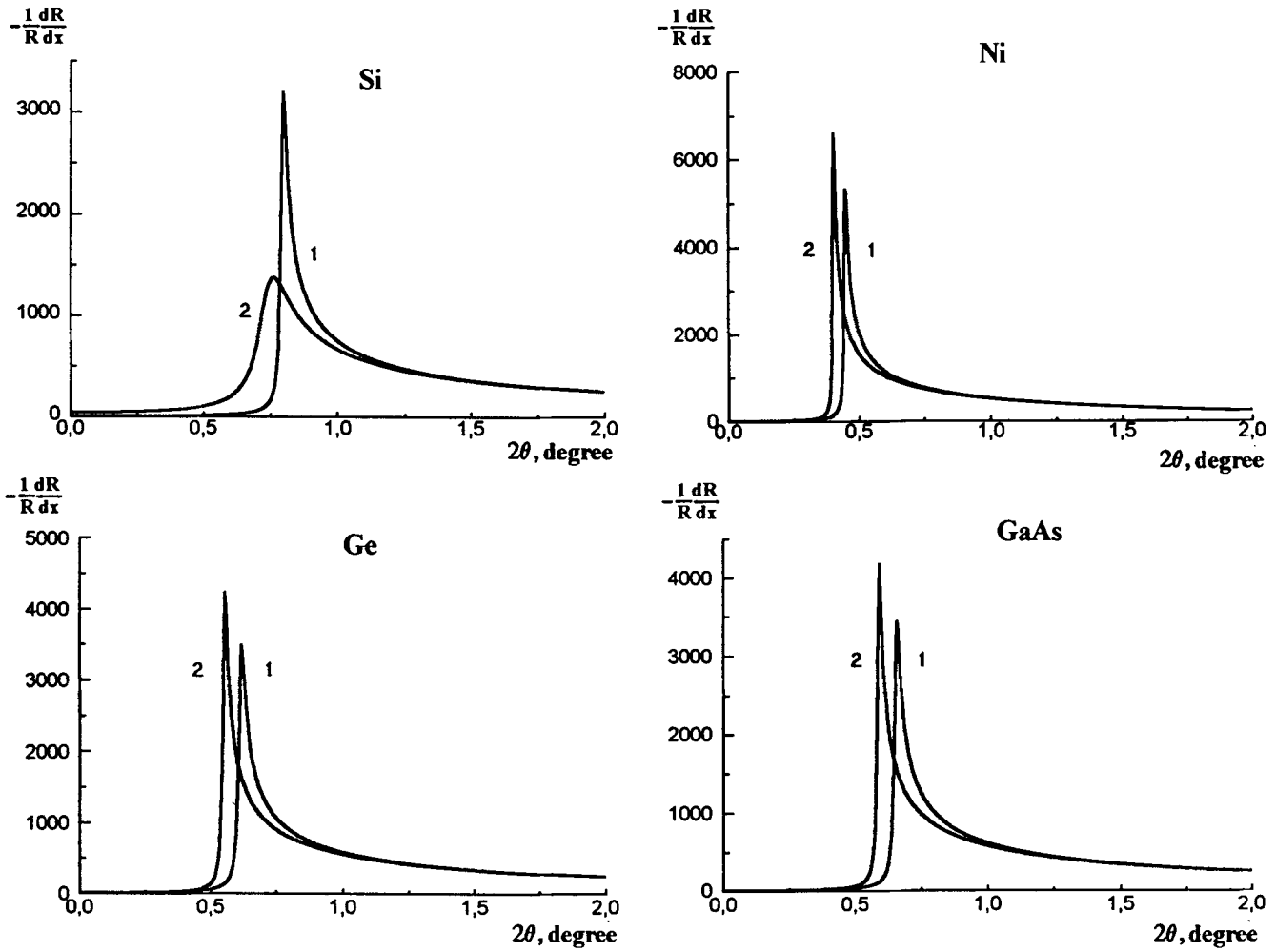

Fig. 6. Examples of derivatives of the Fresnel reflection coefficients for several materials. The calculations were performed for wavelengths of 1.54 Å (curves 1) and 1.39 Å (curve 2).

be attained for $\theta = \theta_m$. In accordance with formula (4) and Fig. 4, the quantities δ and β are expressed in terms of A_m and θ_m as

$$\begin{aligned} \beta &= \frac{4f_0^2}{A_m^2}, \\ \delta &= \sin^2\theta_m - \beta t_0 = \sin^2\theta_m - \frac{12}{A_m^2}. \end{aligned} \tag{8}$$

The matching procedure mentioned in Sec. 2.1 is not needed here at all. Figure 6 shows the logarithmic derivatives of the reflection coefficients for various materials. In contrast to the reflection coefficients (cf. Fig. 1), the quantity $\frac{1}{R}\frac{dR}{d(\sin\theta)}$ is heavily dependent on the angle. Therefore, this dependence can be used not only to determine the material's optical constants, but also to analyze thin films and to study the structure of near-surface layers.

Figures 7–9 show the logarithmic derivatives of reflection coefficients for film–substrate systems identical to those in Figs. 2–4. The comparison of Figs. 2–4 and Figs. 7–9 makes it possible to draw the following conclusions:

(i) The greater the difference in optical constants of the corresponding materials, the higher the sensitivity of the reflectometry data to the presence of a film on the substrate;

(ii) Measurement of the logarithmic derivative $\frac{1}{R}\frac{dR}{d(\sin\theta)}$ (rather than the reflection coefficient itself) enhances the sensitivity of reflectometry in almost all cases;

(iii) The minimal film thickness that can be detected and measured is approximately 5–10 Å for Ni on Si, 20–30 Å for GeO on Ge, and 80–100 Å for SiO_2 on Si.

3. Two-Wavelength Method

3.1. Large Difference in Wavelengths

We now consider another possibility of acquiring data on the properties of solids and solid thin films. The case in point is a measurement of the ratio of reflection coefficients for two wavelengths, i.e.,

$$A(x) = \frac{R(\lambda)}{R(\lambda_1)} = \frac{R(x,z)}{R(x,z_1)}, \tag{9}$$

where z and z_1 are the values of optical constants for the wavelengths λ and λ_1 [see (1)]. Such measurements were first performed in [13] at the wavelengths of CuK_α and CuK_β x-ray lines. The corresponding angular dependences $A(x)$ for various materials have a quite specific form (see Fig. 10), which could also be expected from Fig. 1. The ratio $A(x)$, as well as the logarithmic derivative $\frac{1}{R}\frac{dR}{d(\sin\theta)}$ (see Sec. 2.2), features a rather sharp peak in the vicinity of the critical angle. As a result, the sensitivity to the appearance of thin films at the sample's surface increases.

The results of calculations of the ratio $A(x)$ [see (9)] for the CuK_α and CuK_β lines of the materials of interest with thin films are shown in Figs. 11 and 12. It is evident that, as in the case of the derivative $\frac{1}{R}\frac{dR}{d(\sin\theta)}$ (see Figs. 7–9), the parameters of the films with thickness larger than 10 Å can be measured. This method is especially convenient if the step in absorption of the material under study is located between the lines λ and λ_1 (for example, as in the case of Ni for the lines of CuK_α and CuK_β). The results of measurements for this case are discussed in Sec. 4. It is worth noting here that in the case of SiO_2 film on Si, which is comparatively unfavorable for the reflectometry based on the measurements of $R(\theta)$ and $\frac{1}{R}\frac{dR}{d(\sin\theta)}$ (see Sec. 2), the measurement of the ratio $R(\lambda)/R(\lambda_1)$ makes it possible to enhance the sensitivity of the method, so that it becomes possible to deal with films 50–60 Å thick.

3.2. Closely Spaced Wavelengths

If the wavelengths used in the measurements of the ratio $A(x)$ of reflection coefficients differ little, the optical constants are also little different. In this case, using the expansion

$$R(x,z_1) \approx R(x,z) + (z_1 - z)\frac{\partial R}{\partial z},$$

we can conveniently express the ratio $A(x)$ as

$$A(x) = 1 - 2\,\mathrm{Re}\left[\frac{(z_1 - z)}{R}\frac{\partial R}{\partial z}\right] = 1 - 2x\,\mathrm{Re}\left[\frac{z_1 - z}{z\sqrt{x^2 + z}}\right], \qquad x = \sin\theta\,. \tag{10}$$

In deriving (10), it was taken into account that

$$\frac{\partial R}{\partial z} = \frac{xR}{z\sqrt{x^2 + z}}\,.$$

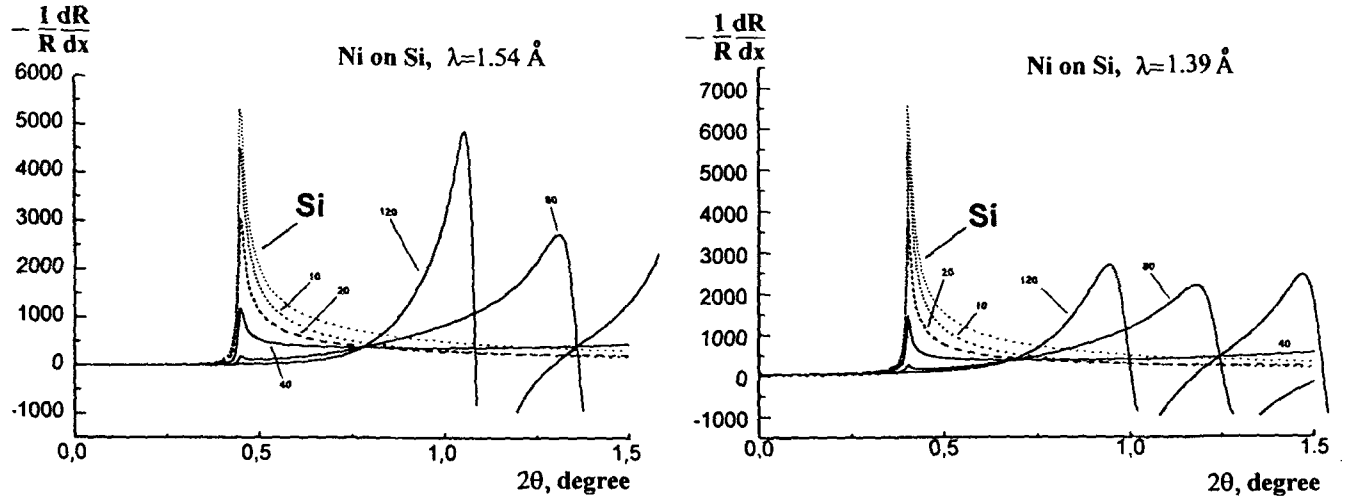

Fig. 7. Examples of derivatives of the Fresnel reflection coefficients for Ni films on Si monocrystal. The numbers at the curves correspond to the films' thicknesses in Å.

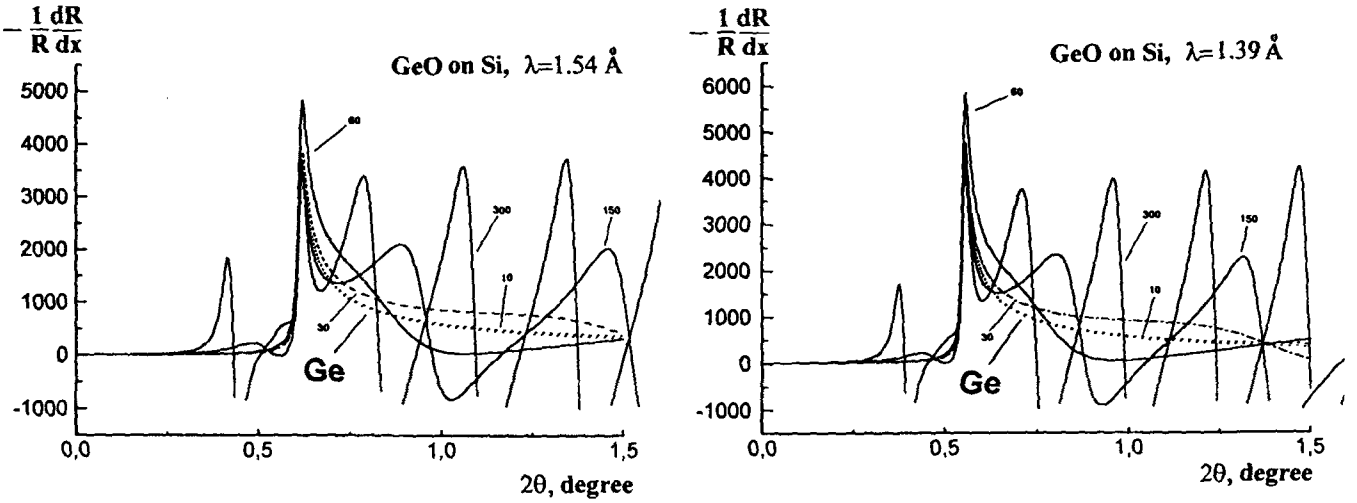

Fig. 8. Examples of derivatives of the Fresnel reflection coefficients for GeO films on Ge monocrystal. The numbers at the curves correspond to the films' thicknesses in Å.

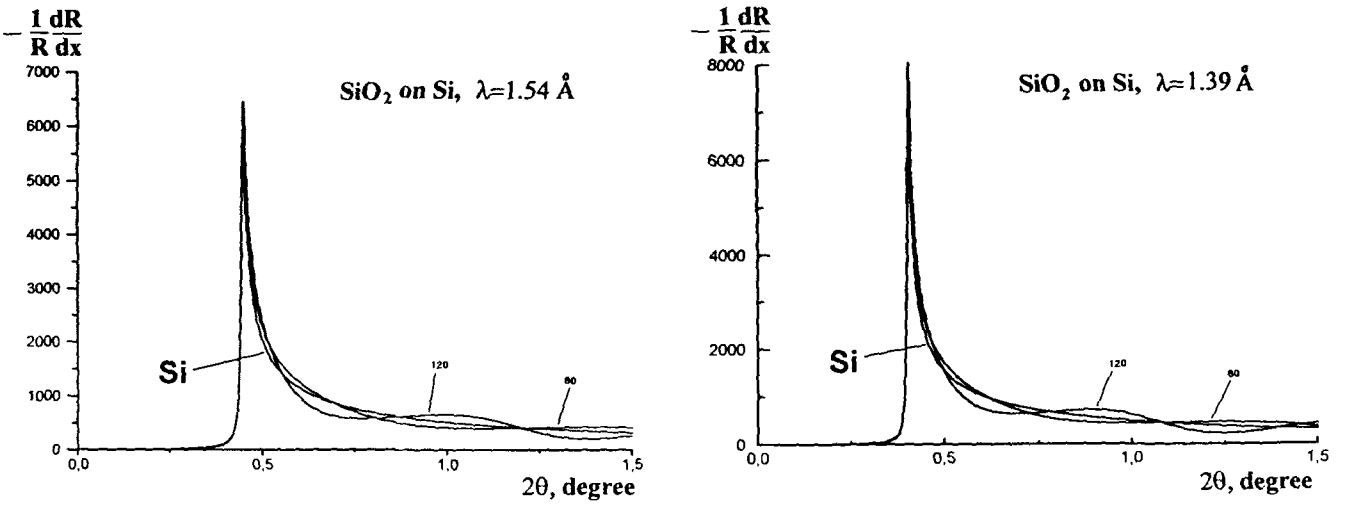

Fig. 9. Examples of derivatives of the Fresnel reflection coefficients for SiO_2 films on Si. The numbers at the curves correspond to the films' thicknesses in Å.

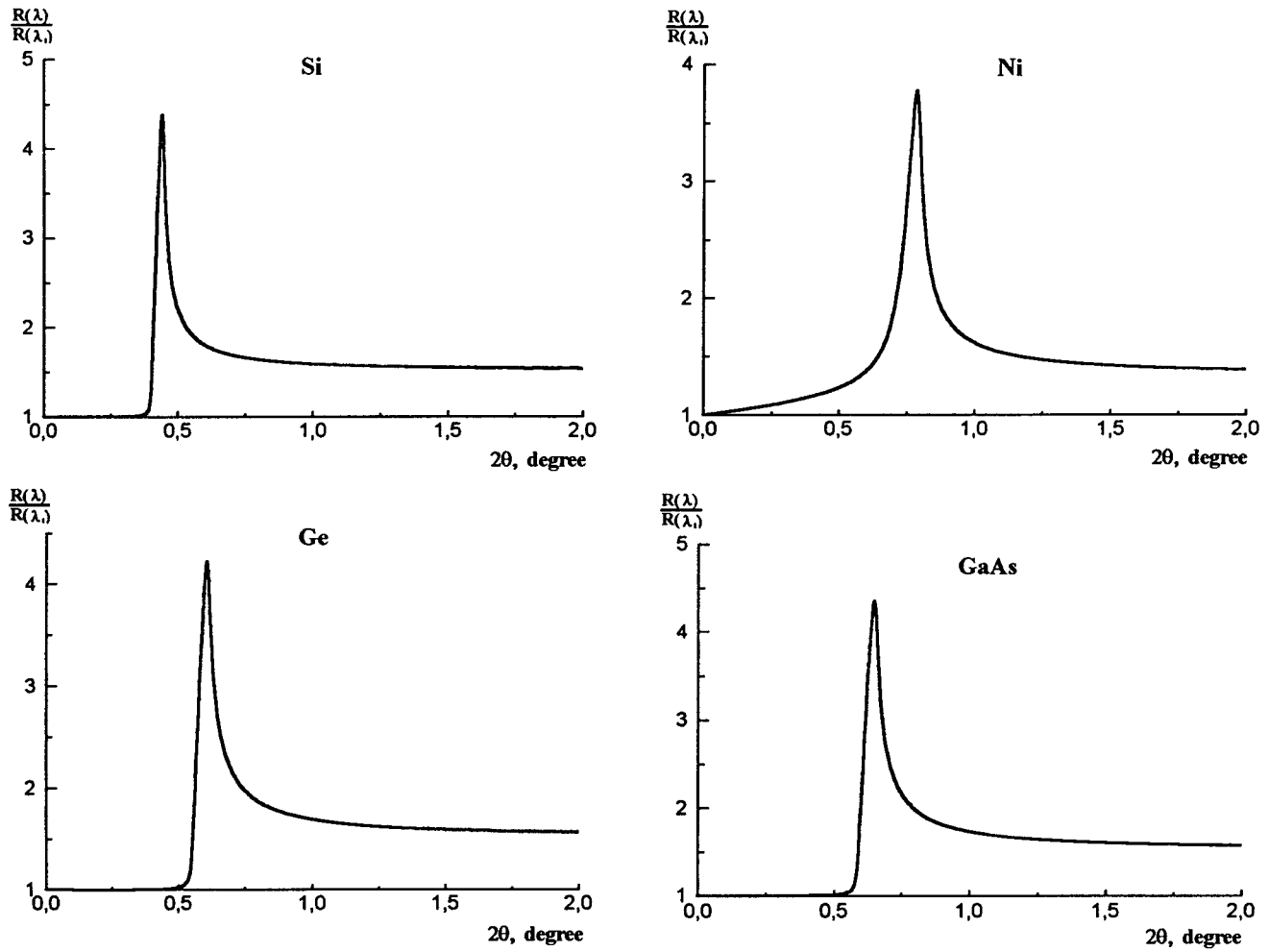

Fig. 10. Examples of the reflection-coefficient ratios for wavelengths of $\lambda = 1.54$ Å and $\lambda_1 = 1.39$ Å for several materials.

Introducing (as in Sec. 2.2) the variable $t = \frac{x^2-\delta}{\beta}$ instead of the angle θ, we arrive at

$$A(x) = 1 - 2\frac{x}{\sqrt{\beta}}\mathrm{Re}\left[\frac{z_1 - z}{z}\frac{1}{\sqrt{t+i}}\right]. \tag{11}$$

Inserting then

$$z_1 - z \approx (\lambda_1 - \lambda)\left[-\frac{d\delta}{d\lambda} + i\frac{d\beta}{d\lambda}\right]$$

in (11), we finally obtain

$$A(x) = 1 - \frac{x}{\sqrt{\beta}}(\lambda_1 - \lambda)\phi(t)\,, \qquad \phi(t) = 2\,\mathrm{Re}\left[\frac{-\frac{d\delta}{d\lambda} + i\frac{d\beta}{d\lambda}}{-\delta + i\beta}\frac{1}{\sqrt{t+i}}\right]. \tag{12}$$

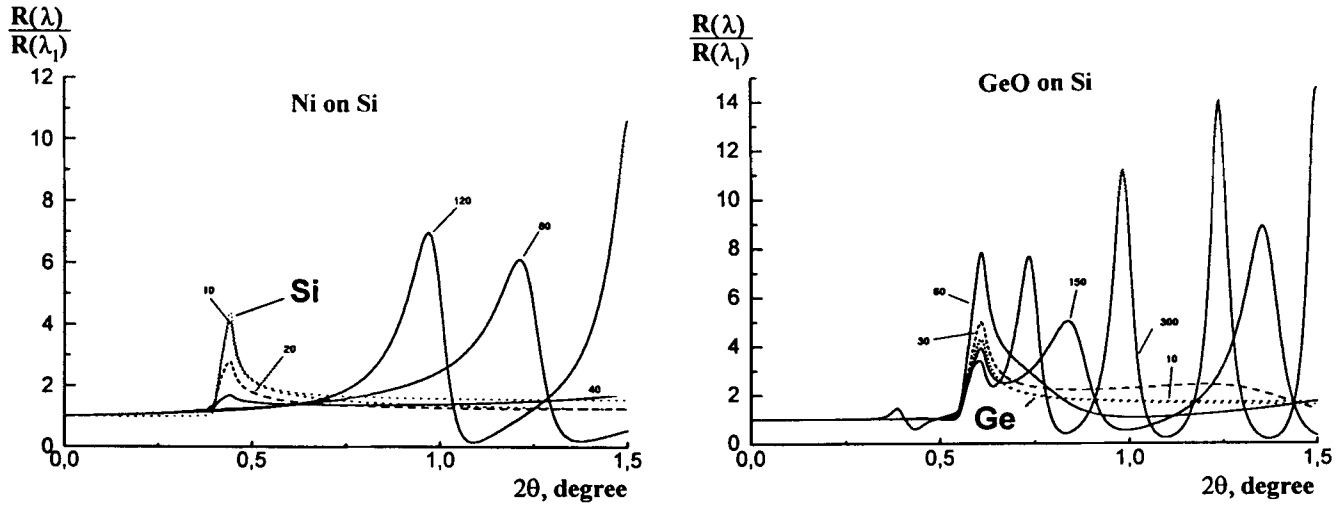

Fig. 11. Examples of the reflection-coefficient ratios for $\lambda_1 = 1.39$ Å and $\lambda = 1.54$ Å for two combinations of film–substrate. The numbers correspond to the film's thickness in Å.

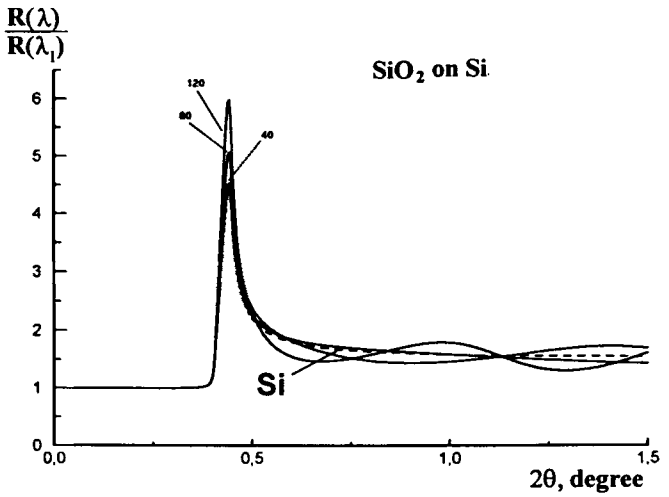

Fig. 12. Examples of the reflection-coefficient ratios for $\lambda_1 = 1.39$ Å and $\lambda = 1.54$ Å for SiO_2 films on Si. The numbers correspond to the film's thickness in Å.

Similarly to the function $f(t)$ in Sec. 2.2, the function $\phi(t)$ features a peak in the vicinity of the critical angle. The position of this maximum is given by

$$t_0 = i\frac{1+y}{1-y}, \qquad y = \left(-\frac{\dfrac{d\delta}{d\lambda} + i\dfrac{d\beta}{d\lambda}}{\dfrac{d\delta}{d\lambda} - i\dfrac{d\beta}{d\lambda}} \times \frac{\delta - i\beta}{\delta + i\beta} \right)^{2/3}. \tag{13}$$

The width of the peak is approximately defined as

$$\frac{\Delta\theta}{\theta_0} \approx \frac{\beta}{\delta}.$$

From the measurement of the ratio of reflection coefficients for closely spaced wavelengths it is basically possible to determine the derivatives of the optical constants δ and β with respect to wavelengths or

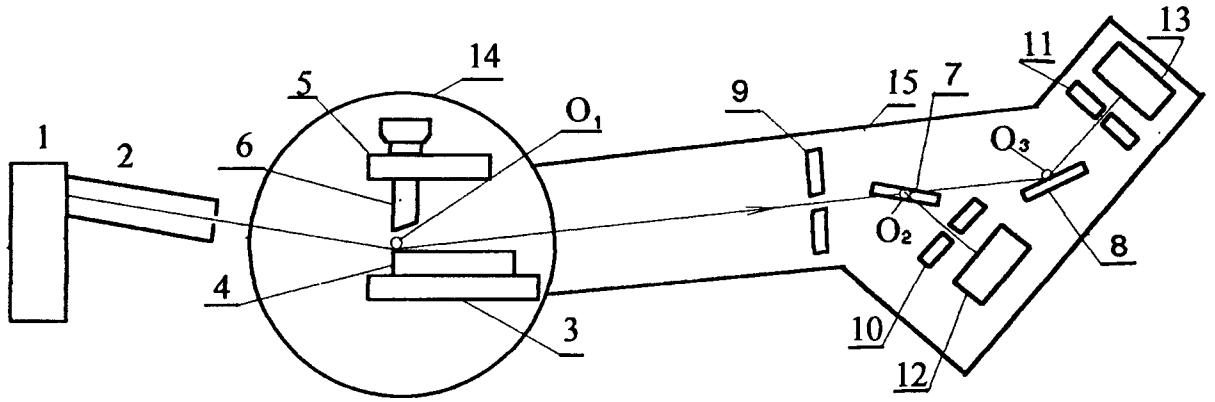

Fig. 13. Schematic diagram of an x-ray reflectometer: 1) x-ray tube; 2) collimator; 3) sample holder; 4) sample; 5) device for the shield translation; 6) absorbing shield; 7) semitransparent monochromator made of pyrolytic graphite; 8) accessory monochromator; 9), 10), and 11) slits; 12) and 13) detectors; 14) rotating table of the goniometer; 15) rotating arm.

frequencies.

4. Experimental Setup and the Results of Measurements

In order to implement the method of measurements outlined above, we used a two-wavelength x-ray reflectometer, first described in [13]. The general layout of the x-ray optical system of this reflectometer is shown in Fig. 13. The reflectometer is equipped with a high-voltage generator and a goniometer from a DRON-3M x-ray diffractometer. As a radiation source, a BSV-22 x-ray tube with Cu cathode was used. The size of the apparent projection of the x-ray focus was 8×0.04 mm. A specially designed sample holder was mounted along the principal axis of the goniometer; this holder included a device for micrometric translation of a defining screen that ensured adjustment of the gap between the holder's end and the sample's surface.

The key element of the goniometer is a facility for splitting the beam under analysis and selecting the spectral lines (see Figs. 14 and 15). Rotating heads 16 and 17 of monochromators 7 and 8 are mounted in the holes of the supporting plate 18 that can be moved in the plane normal to the beam in two mutually perpendicular directions. The rotation axes of two supporting guides 19 and 20 accommodating the scintillation detectors are aligned with the axes of heads 16 and 17. The first monochromator encountered by the x-ray beam is a plate of pyrolytic graphite with an area of 6×15 mm and a thickness of 46 μm. When the first monochromator is rotated to the Bragg diffraction angle $\theta_B = 13.2°$ (the CuK_α line), the peak reflection coefficient of the plate for CuK_α and the transmission coefficient for CuK_β are equal to 22 % and 85 %, respectively. The half-width of the rocking curve of the pyrolytic-graphite plate for a fixed position of the detector is 0.49°. Special design features of the sample holder, the two-channel electron detection, and other elements of the system are described in more detail in [14].

It is noteworthy that modern technologies for the growth and treatment of single crystals with the use of ion implantation make it possible to produce Si wafers with thickness < 5 μm. This would suffice to transmit radiation with a wavelength of 0.1–0.15 nm through the crystal and select a narrow band in the diffraction spectrum. In this case, choosing narrow-bandpass Si monochromators, we can tune each of them to the doublet of lines $K_{\alpha 1}$ and $K_{\alpha 2}$, for which the difference in wavelengths does not exceed 0.5 %. This

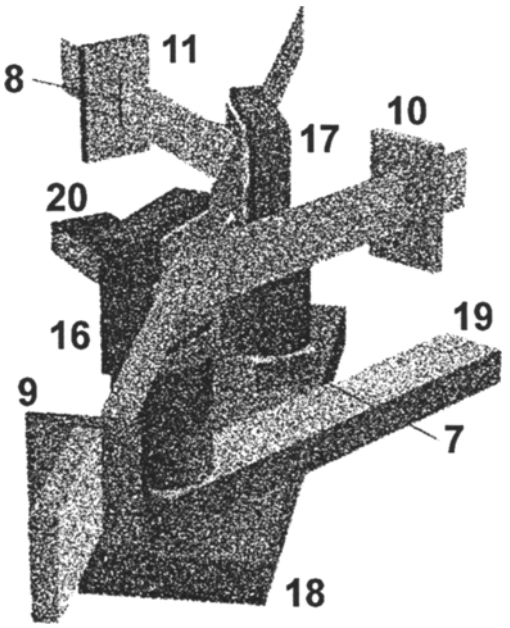

Fig. 14. The scheme of splitting of the beam when it passes through semitransparent monochromators: 9), 10), and 11) slits; 16) and 16) rotating heads; 7) and 8) monochromators; 18) supporting plate; 19) and 20) supporting guides for the detectors.

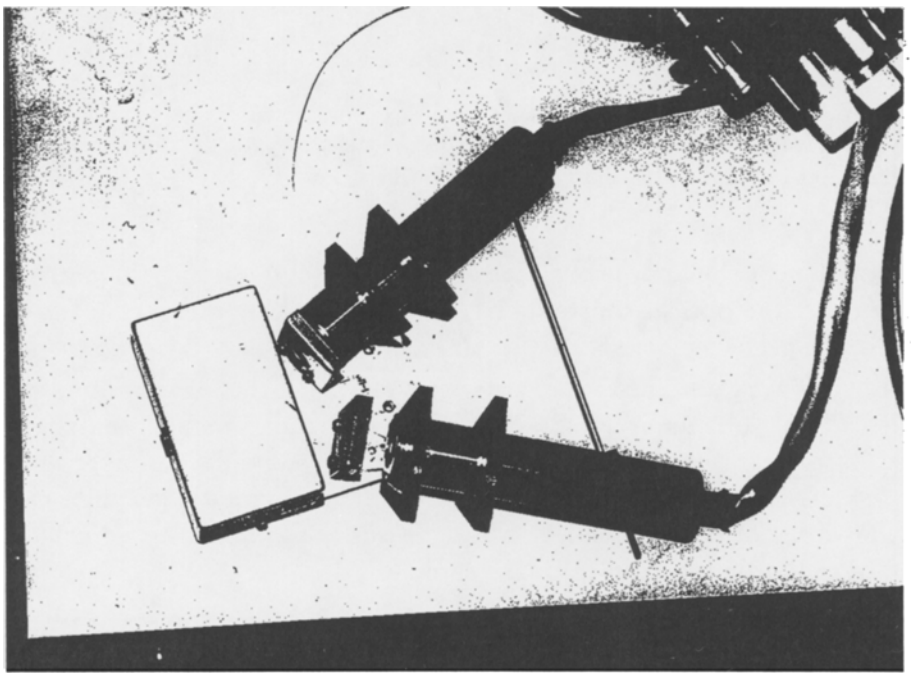

Fig. 15. External view of an x-ray beam splitter with x-ray radiation detectors.

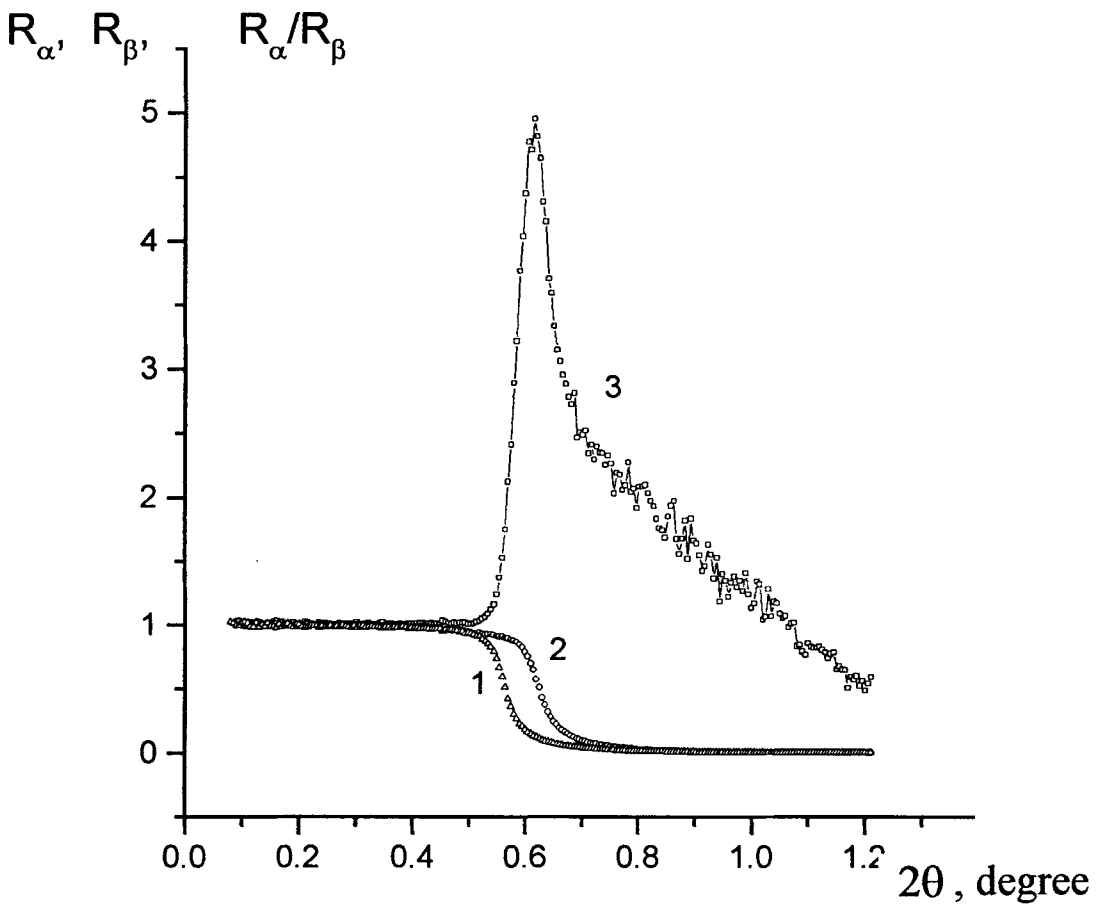

Fig. 16. Angular dependences of reflection coefficients for GaAs single crystal: 1) for the CuK$_\beta$ line, 2) for the CuK$_\alpha$ line, and 3) ratio of reflection intensities for the CuK$_\alpha$ and CuK$_\beta$ lines.

makes it possible to implement the above-considered method for determining the derivatives of the reflection coefficient $dR(\theta,\lambda)/d\lambda$ and the optical constants $d\delta/d\lambda$ and $d\beta/d\lambda$ by measuring the ratio of the reflection coefficients for two wavelengths (see Sec. 3.2).

The results given below were obtained when the first and second monochromators were tuned to the lines CuK$_\alpha$ (0.154 nm) and CuK$_\beta$ (0.139 nm), respectively. For the second monochromator, a pyrolytic-graphite plate was used; this plate constituted an accessory to a DRON-3M diffractometer, had the peak reflection coefficient $R_p(\mathrm{CuK}_\alpha) = 30\,\%$, and was 1-mm thick. The use of two pyrolytic-graphite monochromators makes it possible to vary the width of entrance slit 9, which, in turn, allows one to adjust the angle of collection during the detection of radiation reflected from the sample.

Figure 16a shows the experimental and calculated angular dependences of the reflection coefficient $R^\alpha(\theta)$ and $R^\beta(\theta)$ and the ratio $R^\alpha(\theta)/R^\beta(\theta)$ for an optically polished GaAs wafer. The absence of interference modulation in curves $R^\alpha(\theta)/R^\beta(\theta)$ indicates that the oxide layer is not uniform in thickness and the transition of $\epsilon(z)$ between the oxide and pure GaAs is diffuse.

Figure 17 shows the angular dependences $R^\alpha(\theta)$, $R^\beta(\theta)$, and $R^\alpha(\theta)/R^\beta(\theta)$ for a multilayer heterostructure fabricated by molecular-beam epitaxy on a Si single-crystalline substrate. For the sake of convenience of

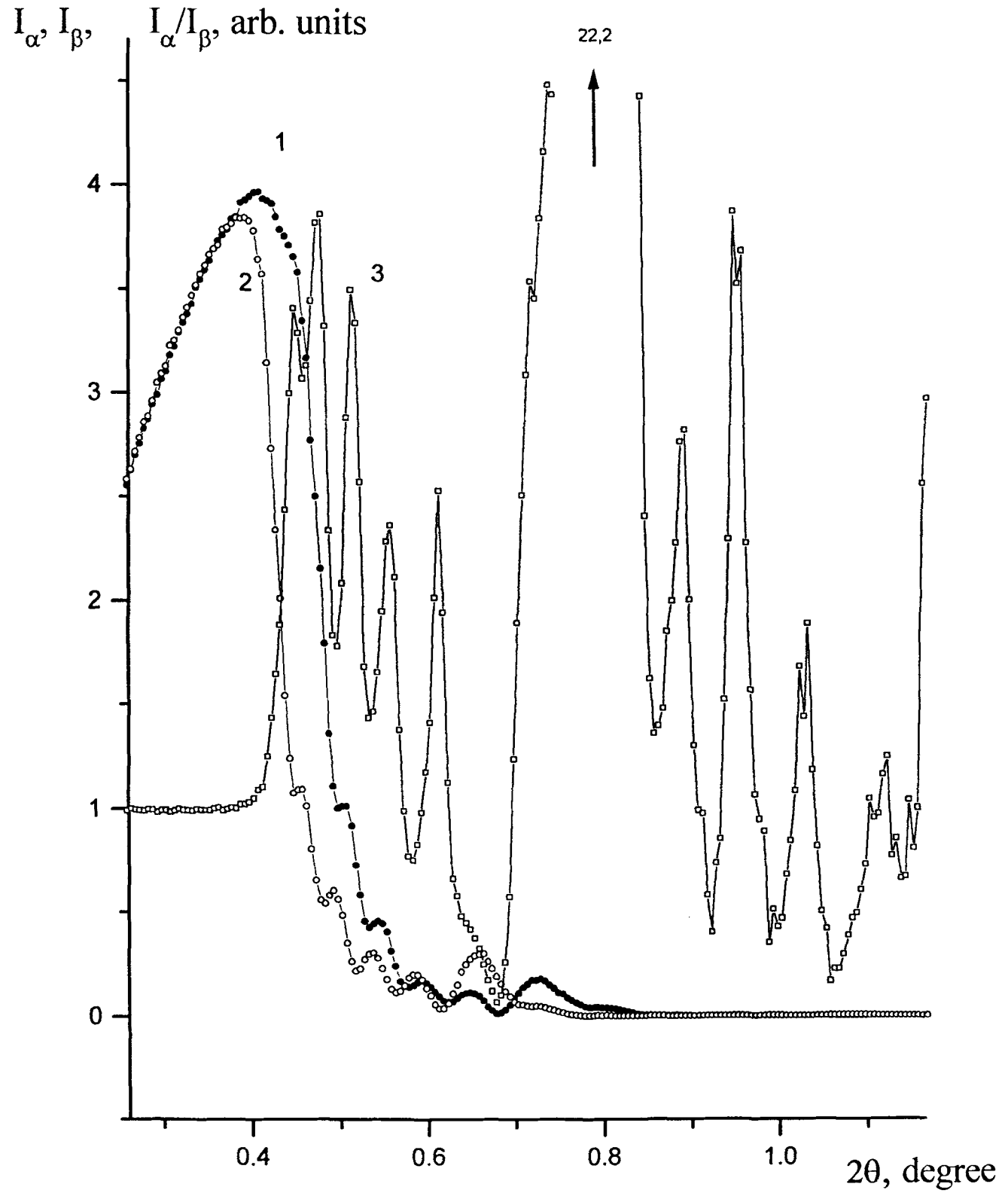

Fig. 17. Angular dependences of specular reflection by $Ge_{0.25}Si_{0.75}-Si$ multilayer structure formed by molecular-beam epitaxy on Si substrate (the period d = 12 nm with d_{Si} = 8 nm): 1) for the CuK_β line, 2) for the CuK_α line, and 3) ratio of reflection intensities for the CuK_α and CuK_β lines (the ratio was normalized to unity for $\theta \to 0$).

comparison, the dependences $R^{\alpha}(\theta)$ and $R^{\beta}(\theta)$ are plotted using a scale factor of three. The heterostructure contains seven periods formed by alternating layers of $GeO_{0.25}SiO_{0.75}$ and pure Si with thicknesses of 4 and 8 nm, respectively; the uppermost layer is made of Si. As is evident from Fig. 17, the division of $R^{\alpha}(\theta)$ and $qR^{\beta}(\theta)$ drastically emphasizes any special features in the curves $R^{\alpha}(\theta)$ and $R^{\beta}(\theta)$. Furthermore, we should stress that the ratio $R^{\alpha}(\theta)/R^{\beta}(\theta)$ (in contrast to the derivative $dR(\theta)/d(\theta)$) does not involve any errors related to instrumental fluctuations in the intensity of the incident x-ray beam because the ratio of the fluorescence yield for the CuK_{α} and CuK_{β} lines at the anode of the x-ray tube is almost independent of the oscillation of the current and high voltage.

5. Conclusion

In this paper, we suggested and tested new methods of x-ray reflectometry; these methods make it possible to enhance the sensitivity and reduce the time required for measuring the parameters of a homogeneous medium and the near-surface layer. These requirements are dictated by the modern level of development of x-ray optical systems and by the potentialities of x-ray sources.

The methods suggested here can be used at the early stage of an experiment prior to film deposition on mirror polished substrates or prior to the growth of crystalline heterostructures.

Weak perturbations of the angular dependence of the reflection coefficient can be conveniently studied by analyzing its derivative; however, this requires a high intensity of the x-ray beam (in order to suppress the noise interferences related to the derivative) and well-controlled conditions of measurements that eliminate influence of instrumental factors.

Analysis of perturbations in the angular dependence of the reflection coefficient on the basis of the ratio of the reflectivities for two close characteristic lines generated by the anode of the x-ray tube is the most efficient.

Optimal conditions for implementation of the methods above-considered are ensured with the use of a two-wavelength x-ray reflectometer equipped with a semitransparent monochromator and suggested first in [13]. According to the measurements conducted in the relative mode, the two-wavelength scheme almost completely eliminates the influence of the drift of electrical parameters of the x-ray generator and uncontrolled variations in the geometry of the experiment. As a result, the thickness of the near-surface layer under study can be reduced to ~ 1 nm.

Acknowledgments

We thank Prof. Yu. V. Kopaev and Prof. A. V. Popov for encouragement and participation in discussions of the results.

This work was supported by the Russian Foundation for Basic Research under Project No. 97-02-17870 and INTAS under Project No. 96-0128.

References

1. L. G. Parrat, *Phys. Rev.*, **95**, 359 (1954).
2. N. Wainfan, N. J. Scott, and L. G. Parrat, *J. Appl. Phys.*, **30**, 1504 (1959).
3. L. Nevot and P. Croce, *J. Appl. Cryst.*, **8**, 304 (1975).
4. O. Renner, *Czech. J. Phys.*, **22**, 1007 (1972).
5. I. F. Mikhailov, S. S. Borisova, L. P. Fomina, and I. N. Babenko, *Proc. SPIE*,**2253**, 186 (1995).
6. J. Cao, M. Yanagihara, M. Yamamoto, Y. Goto, and T. Namioka, *Appl. Opt.*, **33**, 2013 (1994).

7. I. A. Artioukov, V. E. Acadchikov, and I. V. Kozhevnikov, *J. X-Ray Sci. Technol.*, **6**, 223 (1996).
8. S. S. Andreev, S. V. Gaponov, N. N. Slaschenko, et al., *Proc. SPIE*, **3406**, 20 (1998).
9. C. P. J. Barty, "Ultrafast hard x-ray sources and applications," in: *Proceedings of the Sixth international Conference on X-Ray Lasers (Kyoto, 1998).*
10. A. V. Vinogradov (ed.), *Mirror X-Ray Optics* [in Russian], Mashinostroenie, Leningrad (1989).
11. L. K. Izraileva and I. B. Borovskii, *Izv. Akad. Nauk SSSR, Ser. Fiz.*, **36**, 438 (1972).
12. E. Spiller, *Soft X-Ray Optics*, SPIE Publ., Bellingham, Washington (1994).
13. A. G. Tur'yanskii, A. V. Vinogradov, and I. V. Pirshin, *RF Inventor's Certificate* No. 2104481 (1998), MKI G01B 15/08.
14. A. G. Touryanski, A. V. Vinogradov, and I. V. Pirshin, *Prib. Tekh. Éksp.*, No. 1 (1999) (in press).